J Mater Sci: Mater Med (2015) 26:197
DOI 10.1007/s10856-015-5523-2

BIOCOMPATIBILITY STUDIES

# Degradation and silicon excretion of the calcium silicate bioactive ceramics during bone regeneration using rabbit femur defect model

**Kaili Lin[1] · Yong Liu[2] · Hai Huang[2] · Lei Chen[1] · Zhen Wang[2] · Jiang Chang[1]**

Received: 24 October 2014 / Accepted: 8 May 2015 / Published online: 23 June 2015


**Abstract** The investigation of the bone regeneration ability, degradation and excretion of the grafts is critical for development and application of the newly developed biomaterials. Herein, the in vivo bone-regeneration, biodegradation and silicon (Si) excretion of the new type calcium silicate ($CaSiO_3$, CS) bioactive ceramics were investigated using rabbit femur defect model, and the results were compared with the traditional β-tricalcium phosphate [β-$Ca_3(PO_4)_2$, β-TCP] bioceramics. After implantation of the scaffolds in rabbit femur defects for 4, 8 and 12 weeks, the bone regenerative capacity and degradation were evaluated by histomorphometric analysis. While urine and some organs such as kidney, liver, lung and spleen were resected for chemical analysis to determine the excretion of the ionic products from CS implants. The histomorphometric analysis showed that the bioresorption rate of CS was similar to that of β-TCP in femur defect model, while the CS grafts could significantly stimulate bone formation capacity as compared with β-TCP bioceramics ($P < 0.05$). The chemical analysis results showed that Si concentration in urinary of the CS group was apparently higher than that in control group of β-TCP. However, no significant increase of the Si excretion was found in the organs including kidney, which suggests that the resorbed Si element is harmlessly excreted in soluble form via the urine. The present studies show that the CS ceramics can be used as safe, bioactive and biodegradable materials for hard tissue repair and tissue engineering applications.

## 1 Introduction

Bone replacements are frequently required to substitute the damaged hard tissues due to trauma, disease or surgery [1, 2]. Recently, the calcium silicate ($CaSiO_3$, CS) ceramics and their composites are investigated as potentially new type of bioceramics for bone regeneration and bone tissue engineering applications [2–14]. Previous studies have confirmed that the CS bioceramics possess excellent bioactivity and biodegradability [12], and in vitro cell culture studies have shown that the CS bioceramics well supported the attachment and proliferation of bone marrow mesenchymal stem cells (BMSCs) and osteoblasts [11, 13, 15], and the bioactive Si ions released from CS provided a preferable extracellular environment for directing BMSCs proliferation and differentiation toward the osteogenic lineage [9], and enhancing the proliferation and angiogenesis process of the human umbilical vein endothelial cells (HUVECs) [3]. Our in vivo studies have revealed that CS and its composites enhanced new bone formation as compared with traditionally clinical used β-tricalcium phosphate (β-TCP) bioceramics [2, 3]. Moreover, no acute inflammation reaction was observed at the interface between the host tissues and CS grafts [2]. The study also showed that the CS possessed excellent degradability in vivo and the cell-mediated process involved in the

Kaili Lin and Yong Liu are Co-first authors.

✉ Zhen Wang
wangzhen@fmmu.edu.cn

✉ Jiang Chang
jchang@mail.sic.ac.cn

[1] State Key Laboratory of High Performance Ceramics and Superfine Microstructure, Shanghai Institute of Ceramics, Chinese Academy of Sciences, Shanghai 200050, China

[2] Institute of Orthopedic Surgery, Xijing Hospital, Fourth Military Medical University, Xi'an 710032, China

degradation of CS bioceramics [2]. However, no study has been reported on the metabolism of the degraded products, in particular the Si component.

Though silicon (Si) is a major component in soil environment, it is a trace element in human and animal tissues. Si is most abundant in connective tissue, bone, tendon, muscle, hair, feather and skin [16, 17]. Si is also a constituent of certain glycosaminoglycans and polyuronides, where it occurs firmly bound to the polysaccharide matrix [18]. As for humans, Si concentrations range from 0.6 ppm for serum to 41 ppm for muscle, and to a high of 57 ppm for lung tissue. In other species such as rats and monkeys, the Si concentrations are similar to humans, around 25 ppm in femora and <1 ppm in serum [16, 17, 19–21].

It is generally considered that the accumulation of the trace elements including Si in body can bring about serious toxicity. For example, the rapid death in mice by nephrosis was confirmed after injection the silica-containing ceramic powders [16, 22, 23], and the mortality rate was directly correlated to silica content of the materials [24]. As a macroconstituent, the amount of Si component in CS ceramics reaches 24.14 wt%. Therefore, it is necessary to investigate the degradation way of CS as a bone graft, and the distribution of Si in the body during the degradation process, which is a critical issue for clinical security in the development and application of the newly developed biomaterials. In present study, the biodegradation of CS ceramic scaffolds during bone regeneration was investigated using rabbit femur defect model, in which the Si excretion from CS and the distribution of Si component in animal body were traced by chemical analysis of different tissues and body fluids.

## 2 Materials and methods

### 2.1 Preparation and characterization of macroporous ceramic scaffolds

The CS powders were prepared by chemical precipitation method using $Ca(NO_3)_2{\cdot}4H_2O$ and $Na_2SiO_3{\cdot}9H_2O$ as raw materials according to our previous studies [11]. The β-TCP powders for this study were synthesized by the reaction of $Ca(NO_3)_2{\cdot}4H_2O$ with $(NH_4)_2HPO_4$ [10]. The obtained CS and β-TCP powders were sieved to obtain the powders with particulate size less than <160 μm, respectively, and then mechanically mixed with 300–450 μm polyethylene glycol (PEG) particulates at a weight ratio of 45:55. The mixture was dry pressed at a uniaxial pressure of 14 MPa in a stainless steel die to obtain green disks with a diameter of 6 mm and a thickness of 7 mm. To prepare macroporous CS and β-TCP ceramics, the green disks were heat treated at 400 °C for 2 h at a firing rate of 2 °C/min to drive off the porogens, and then were sintered at 1120 and 1100 °C for 3 h, respectively at a firing rate of 2 °C/min. After sintering, the samples were cooled to room temperature in the furnace. Finally, the samples were amended into shape with 5 mm in diameter and 6 mm in thickness.

The cross-section of the macroporous ceramic samples was observed by field emission scanning electron microcopy (FESEM, JSM-6700F, JEOL, Japan). The phases of the samples were examined by X-ray diffraction (XRD, Geigerflex, Rigaku Co., Japan) using mono-chromated CuKα radiation.

### 2.2 Animal experiment

All experimental protocols concerning animals were approved by the Animal Care and Experiment Committee of the Xijing Hospital affiliated to 4th Military Medical University. Before animal surgery, the ceramic samples were sterilized by Gama radiation. Eighteen adult male New Zealand white rabbits were used for this study. All animals were older than 3 months and weighed between 2.0 and 3.0 kg. The animals were anesthetized with an intra-muscular dose of anesthetics (SumianxinzhusheyeII, Jilin, China) at dosage of 0.1–0.15 mL/kg. After proper preparation, the femur bone was exposed through a skin incision approximately 1 cm in length over the linea media. The circular bone defect with a diameter of 5 mm and a depth of 6 mm were made in the femur bone using a trephine on a slow-speed electric handpiece by applying 0.9 % physiologic saline irrigation. After the bone was removed, the defects were grafted with macroporous CS or β-TCP ceramic scaffolds. The closure of subcutaneous tissues was performed with 4/0 Vicryl and the skin was relocated with 4/0 Mersilk continuous sutures, then the antibiotics were administered postoperatively by intramuscular injection.

A special chamber was designed to separate and collect the urine from the feces through a sieve. Our previous study showed that the CS scaffolds possessed fast degradation rate. After implantation of the porous CS scaffolds in rabbit calvarial defects for 8 and 16 weeks, the residual material of CS only remained around 15 and 20 %, respectively. Therefore, the time points at weeks 4, 8 and 12 were selected to examine the degradation and silicon excretion of the CS scaffolds during bone regeneration in present study. The urine and blood samples were obtained at week 4, 8 and 12 after implantation. The blood samples were stored in a refrigerator after coagulation at room temperature. The animals were euthanized at week 4, 8 and 12 after implantation, and the defects with an additional 2-mm surrounding tissue were dissected from the host bone. Then the harvested samples were fixed in a 10 % paraformaladhyde solution buffered by 0.1 M phosphate

solution (pH 7.2) for 2 weeks before further analysis. In addition, at each experiment point, the organs including kidney, liver, lung and spleen were removed and stored by freezing at −80 °C until digestion for chemical analysis.

### 2.3 Histological analysis

The harvested samples were dehydrated in graded series of alcohol (70, 90 and 100 %), and then embedded in polymethyl metacrylate (PMMA) without decalcification. Thin sections with ~200 μm thickness were cut using a microtome (SP1600, Leica, Germany), and then were polished into a thickness of around 50 μm using grinding machine (Exakt-Micro-Grindin System, Leica, Germany).

#### *2.3.1 Histomorphometric analysis*

Three randomly sections of the central part at each sample were used for histomorthometric analysis. The Von-Gieson stained sections were examined under light microscopy (DMLA, Leica). The area of the newly formed bone (NB) and the residual material (RM) were quantitatively evaluated. The NB (%) and RM (%) were calculated as follows [2]:

$$\mathrm{NB}(\%) = \frac{\text{area of newly formed bone in the 5 mm diameter defect}}{\text{total area of the 5 mm diameter defect}} \times 100\%$$

$$\mathrm{RM}\ (\%) = \frac{\text{area of residual material}}{\text{area of pre - implantation material}} \times 100\,\%$$

### 2.4 Si excretion and distribution analysis

The Si excretion pathway of the biodegraded CS scaffolds was determined by monitoring the Si concentrations in the collected urine and blood, while the Si accumulation after the biodegradation of CS scaffolds was analyzed by determination the Si concentrations in the collected organic tissues including lung, liver, kidney and spleen. The results were compared with the control group (β-TCP). The urine, blood and tissue samples were chemically digested in concentrated nitric acid (spectral purity) using a microwave digester [16, 17]. To minimize Si contamination, all samples were microwave digestion using new Teflon vessel as reactor, and the solutions after digestion were stored in plastic wares. The Si concentrations of the samples were determined by inductively coupled plasma atomic emission spectroscopy (ICP-AES, Varian 715ES, USA).

### 2.5 Statistics

Results were expressed as mean ± standard deviation (SD). Statistical software SPSS 11.5 (Chicago, USA) was used to analyze the data by One-Way ANOVA. All results were considered to be significant at the 5 % critical level ($P < 0.05$).

## 3 Results

### 3.1 Characterization of the macroporous CS and β-TCP ceramic scaffolds

Figure 1 shows the FESEM images of the fractured surface of the macroporous CS and β-TCP ceramic scaffolds. It is clear that the fabricated scaffolds were highly porous structures with evenly distributed and interconnected pores. The size of the macropores was in the range of 250–400 μm, and the shape of the pores was similar to that of the PEG porogens. The FESEM observation revealed that the macropores created by porogens had around 15 % shrinkage in size after sintering due to the densification effect [25]. XRD characterization results revealed that the fabricated macroporous scaffolds were composed of pure α-CS and β-TCP phase, respectively (Fig. 2).

### 3.2 Histological analysis

Histological images stained with Von-Gieson showed that the control group (β-TCP scaffolds) had little newly formed bone after operation, while much more newly formed bone was observed in CS group at weeks 4 (Fig. 3a). In addition, the resorption phenomenon in the neighborhood of the implant surfaces was observed, indicating the remodeling process of the bone. With the increase of the implantation period to 8 weeks, more newly formed bone was observed in both groups as compared with the week 4 time point. Comparing with CS group, the newly formed bone was much less in β-TCP group. Furthermore, both of the samples showed higher resorption. Further increase of the implantation periods to 12 weeks, the newly formed bone in CS scaffolds appeared to be in a laminar arrangement (Fig. 3Ac). However, without apparent improvement of the newly formed bone was observed

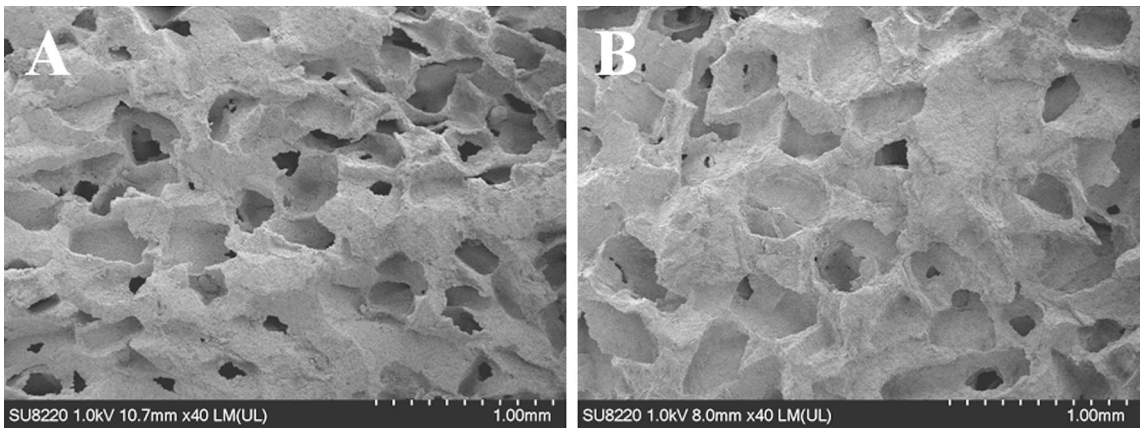


**Fig. 1** FESEM images of the fractured surface of the fabricated macroporous ceramic scaffolds: CS (**a**) and β-TCP (**b**)

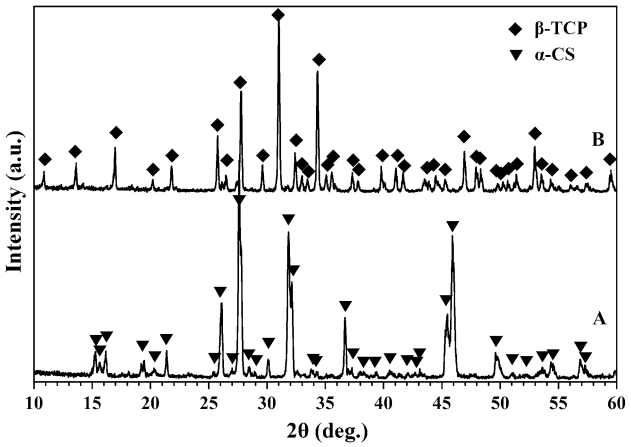


**Fig. 2** XRD patterns of the fabricated macroporous ceramic scaffolds: CS (**a**) and β-TCP (**b**)

in β-TCP group. In addition, it was important to point out that the acute inflammation process was absent at the interface between the tissues and the implanted materials.

Histomorphometric assay further confirmed that the newly formed bone area in CS scaffolds increased significantly with the increase of the implantation periods. As for β-TCP group, newly formed bone area increased apparently with the increase of implantation time from 4 to 8 weeks, while maintained with the further increase of the implantation time to 12 weeks (Fig. 3b). It is clear to see that the percentage of newly formed bone of CS scaffolds is remarkably higher than that of the β-TCP scaffolds. After 4 weeks of implantation, the newly formed bone in CS scaffolds was about 7 % of total area, increased to 19 % at weeks 8, and further increased to 29 % at weeks 12. In contrast, the percentage of newly formed bone in β-TCP scaffolds was lower than that in CS scaffolds. At weeks 4, it only reached 1 %, and 12 and 11 % at weeks 8 and 12, respectively. The results show that the stimulation of the bone-regeneration ability of CS scaffolds was significantly stronger than that of β-TCP bioceramic scaffolds.

Figure 3c confirms that the area of residual materials decreases with the increase of the implantation periods. However, the significant difference between CS and β-TCP was absent, suggesting that the bioresorption rate of CS scaffolds in vivo is similar to that of β-TCP bioceramic scaffolds under rabbit femur defect model.

The concentrations of silicon in urine and blood are presented in Fig. 4. The only significant difference between CS and β-TCP implants was found in urine. In β-TCP group, the silicon concentrations were around 65, 57 and 50 ppm at weeks 4, 8 and 12, respectively after operation, which was significantly lower than those for CS implants (112, 104 and 119 ppm, respectively). Figure 5 shows the concentrations of silicon in the tissues. It is clear to see that without significant difference is found in the main organs including kidney, liver, lung and spleen in whole determination periods.

## 4 Discussion

It is well considered that the suitable biomaterials used for bone tissue repair should be bioresorbable and gradually replaced by the newly formed bone [2]. Moreover, the implants should be biocompatible and the degradation products can be facilely excreted, because the accumulation of the degraded products might bring about serious toxicity. Recent studies suggested that the calcium silicate (CS) ceramics possessed good bioactivity, biodegradability and bone regeneration capacity. However, the excretion and distribution of the CS degradation products have not been reported up to now, which are critical issues for the clinical security of the CS bioceramics. In present study, the biodegradation, Si excretion and distribution during

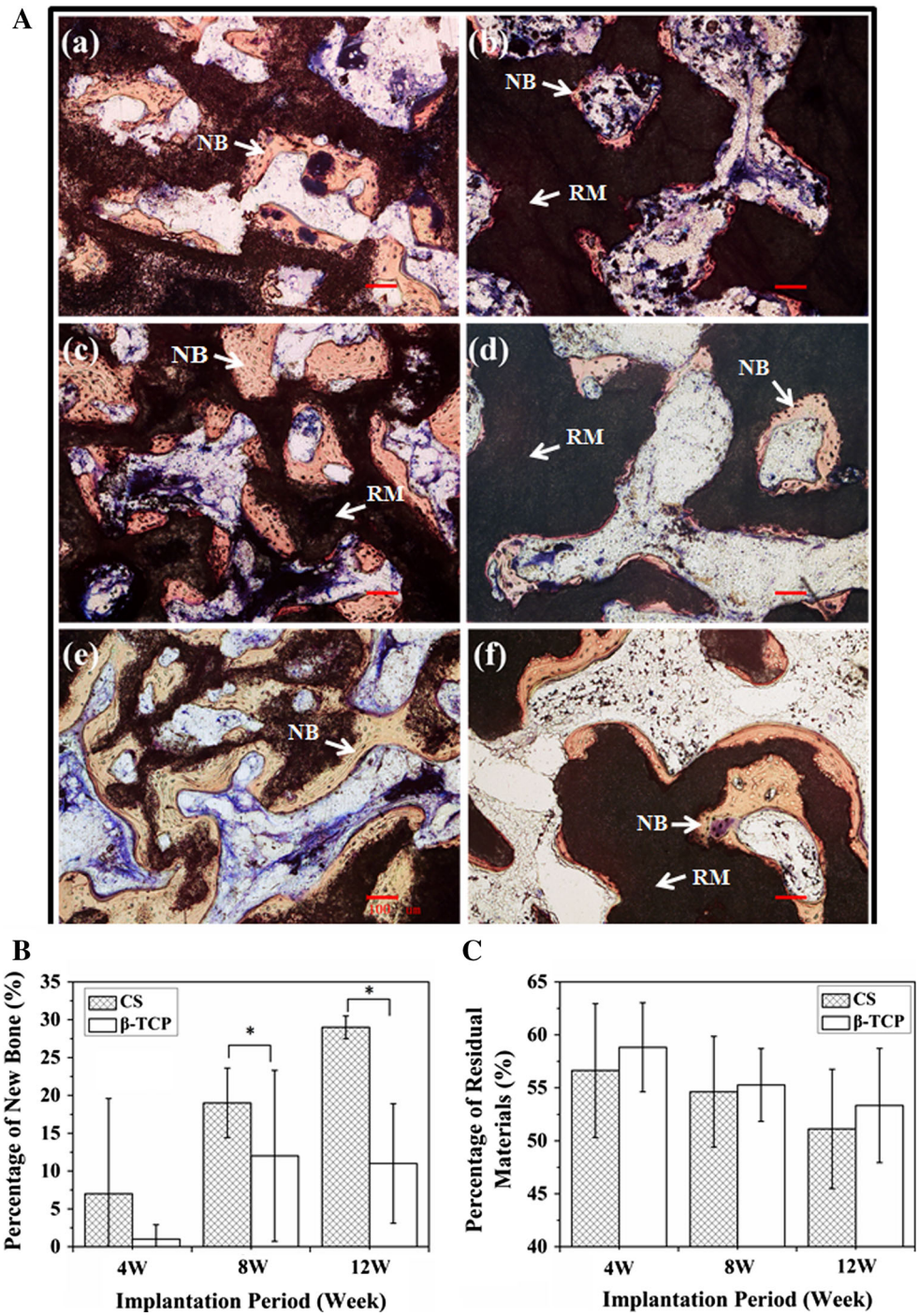


**Fig. 3** Histological images (**A**) of newly formed bone in femur defects after implantation of CS (*a*, *c*, *e*) and control sample β-TCP (*b*, *d*, *f*) for 4 (*a*, *b*), 8 (*c*, *d*) and 12 (*e*, *f*) weeks (Van Gieson's picricefuchsine staining). *NB* newly formed bone, *BM* residual material, *bar* 100 μm; (**B**) and (**C**) are the percentage of new bone area and the residual materials after implantation for different periods, respectively using histomophometric analysis, $^{*}P < 0.05$

bone regeneration were investigated using rabbit femur defect model.

The histomorphometric analysis showed that the percentage of residual material of the implants decreased apparently with the increase of the implantation period, and the degradation rate of CS scaffolds was similar to that of β-TCP bioceramic scaffolds under rabbit femur defect model. The previous study showed that the degradation rate of CS was apparently higher than that of β-TCP under calvarial defect of rabbits. The significant difference of the degradation rate might be due to the different implantation sites. The solubility product constant ($K_{SP}$) of CS ($2.5 \times 10^{-8}$) is much higher than that of β-TCP ($2.0 \times 10^{-29}$), suggesting the faster dissolution rate of CS in aqueous solution comparing with β-TCP. It is considered that the solution-mediated process is one of the main

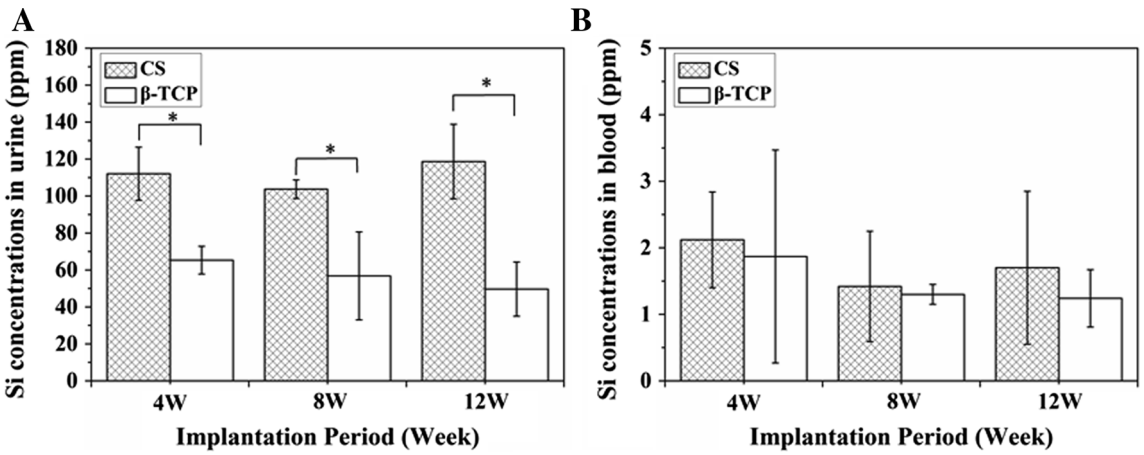


**Fig. 4** The concentrations of silicon in urine and blood collected from the rabbits filling with CS and β-TCP bioceramic scaffolds for 4, 8 and 12 weeks. The concentrations are quantified in ppm wet weight. The significant difference between groups was found in urine

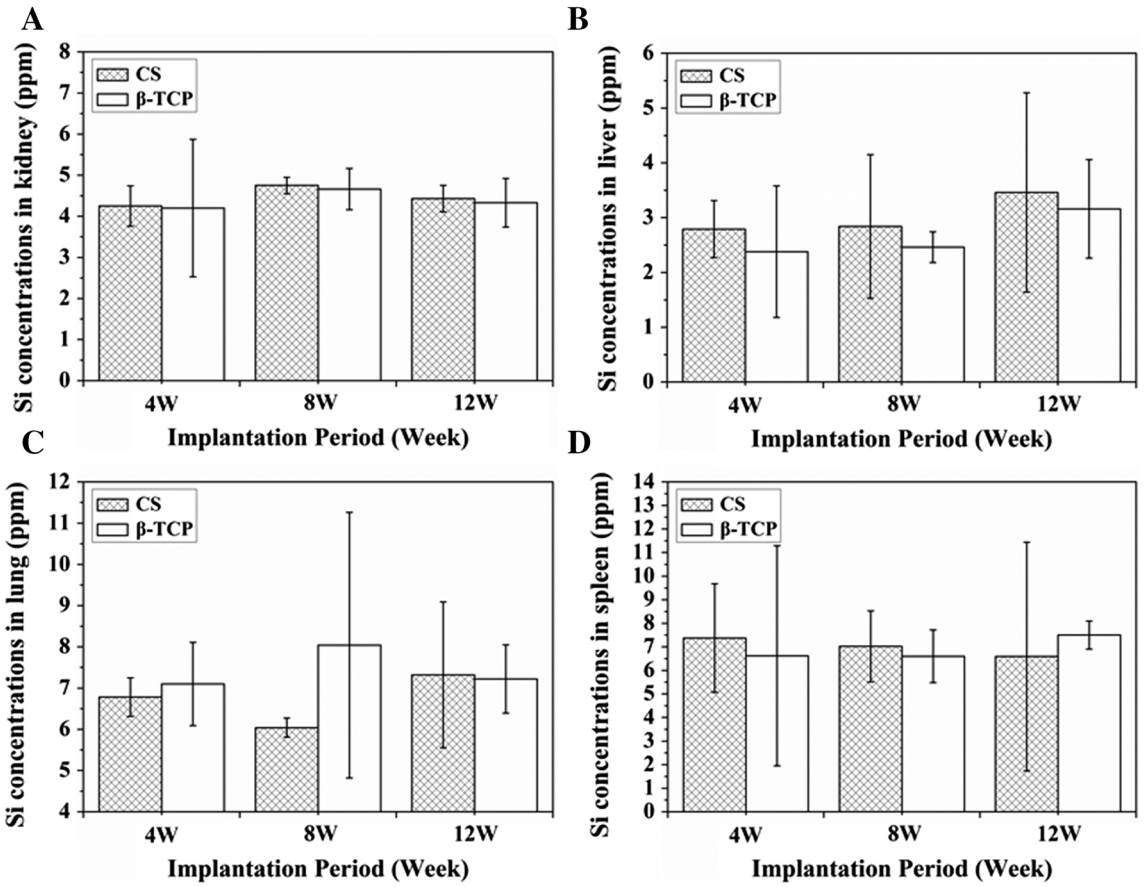


**Fig. 5** The concentrations of silicon in various tissues resected from the rabbits filling with CS and β-TCP bioceramic scaffolds for 4, 8 and 12 weeks. The concentrations are quantified in ppm wet weight. Without significant difference between groups was found

driving forces for the degradation of the biodegradable materials [2]. The calvarial environment possesses abundant blood vessels than the femur model, which might accelerate the excretion rate of the degradation products and ultimately increase the degradation rate of CS in calvarial defects.

The histomorphometric analysis in present study further confirmed our previous finding that the CS can

stimulate new bone formation although the in vivo defect model is different as the previous one [2]. At early stage of regeneration after implantation, the newly formed bone was presented on the surfaces of the CS implants. In contrast, only little amount of new bone formed in the defects filled with β-TCP bioceramic scaffolds. Quantitative analysis showed that although the percentage of newly formed bone in both CS and β-TCP ceramic scaffolds increased with increase of the implantation periods, the percentage of newly formed bone in CS group is significantly higher than that in β-TCP group. After 4, 8 and 12 weeks of implantation, the area of newly formed bone in CS was about 7, 19 and 29 % of total area, respectively, while the area of newly formed bone in β-TCP was only about 1, 12 and 11 % of total area, respectively (Fig. 3c). The better bone regeneration ability of CS ceramics is due to the gradual release of silicon ions into the body fluid during degradation of CS in vivo. The release of silicon from the silicate-based and Si-containing apatite materials can result in a significant up-regulation of osteoblast proliferation, differentiation and bone-related gene expression [8, 9, 26–30]. Previous studies about bone metabolism have also implied that silicon may be allied to the initiation of pre-osseous tissue mineralization, whether in periosteal or in endochondrral ossification. In addition, the silicon can associate with calcium in an early stage of calcification [31].

After implantation of the degradable CS ceramics, the reaction takes place on the surface of the implants when they get in contact with surrounding body fluid, which initiates the dissolving of silicon ions into the body fluid and subsequently diffuses into the urine or bloodstream. This may result in an increase of the silicon concentration and accumulation of the silicon in body organs. However, our results demonstrated that no significant increase of the silicon concentrations was determined in the blood and organs including kidney, liver, lung and spleen in whole analysis periods. The increase of silicon concentration was only observed in urine samples (Fig. 4). Moreover, the silicon concentration in urine was in the range of 104–119 ppm, which was well below saturation (180 ppm) [17]. The results suggested that the degradation product of CS could be filtered by the kidney and was finally excreted through the urine [17]. After implantation of CS in bone defects, the released silicon ions from CS ceramics could be successfully removed from the body, no silicon accumulation in blood and important organs was detected and the silicon concentration in main body organs and body fluids remains within physiologically safe ranges. Our result was similar to the results of the studies on silicate based bioactive glasses, which also showed that silicon ions were not accumulated in blood and important organs [16, 17].

## 5 Conclusions

Herein, the biodegradability and silicon excretion of the macroporous CS ceramic scaffolds during bone regeneration were investigated using rabbit femur defect model, and the results were compared with the traditionally clinical used macroporous β-TCP. The quantitative analysis results showed that CS could significantly stimulate the bone regeneration process comparing with β-TCP in a rabbit femur defects model, while the resorption rate of CS was similar to that of β-TCP under femur defect situation. The silicon ions released from the CS during degradation could be safely excreted through the urine, and no silicon accumulation was found in important body organs and blood. The present study suggests that the CS ceramics may be used as the save, bioactive and biodegradable materials for hard tissue repair and tissue engineering applications.

**Acknowledgments** This work was supported by grants from the Natural Science Foundation of China (Grant No.: 30900299, 81190132 and 51061160499).

## References

1. Lin K, Xia L, Li H, Jiang X, Pan H, Xu Y, et al. Enhanced osteoporotic bone regeneration by strontium-substituted calcium silicate bioactive ceramics. Biomaterials. 2013;34:10028–42.
2. Xu S, Lin K, Wang Z, Chang J, Wang L, Lu J, et al. Reconstruction of calvarial defect of rabbits using porous calcium silicate bioactive ceramics. Biomaterials. 2008;29:2588–96.
3. Wang C, Lin K, Chang J, Sun J. Osteogenesis and angiogenesis induced by porous beta-CaSiO(3)/PDLGA composite scaffold via activation of AMPK/ERK1/2 and PI3K/Akt pathways. Biomaterials. 2013;34:64–77.
4. Liu S, Jin F, Lin K, Lu J, Sun J, Chang J, et al. The effect of calcium silicate on in vitro physiochemical properties and in vivo osteogenesis, degradability and bioactivity of porous beta-tricalcium phosphate bioceramics. Biomed Mater. 2013;8:025008.
5. Lin K, Zhang M, Zhai W, Qu H, Chang J. Fabrication and characterization of hydroxyapatite/wollastonite composite bioceramics with controllable properties for hard tissue repair. J Am Ceram Soc. 2011;94:99–105.
6. Wang C, Chiang T, Chang H, Ding S. Physicochemical properties and osteogenic activity of radiopaque calcium silicate–gelatin cements. J Mater Sci Mater Med. 2014;25:2193–203.
7. Motisuke M, Santos VR, Bazanini NC, Bertran CA. Apatite bone cement reinforced with calcium silicate fibers. J Mater Sci Mater Med. 2014;25:2357–63.
8. Fei L, Wang C, Xue Y, Lin K, Chang J, Sun J. Osteogenic differentiation of osteoblasts induced by calcium silicate and calcium silicate/beta-tricalcium phosphate composite bioceramics. J Biomed Mater Res. 2012;100B:1237–44.
9. Wang C, Xue Y, Lin K, Lu J, Chang J, Sun J. The enhancement of bone regeneration by a combination of osteoconductivity and osteostimulation using beta-CaSiO3/beta-Ca3(PO4)2 composite bioceramics. Acta Biomater. 2012;8:350–60.
10. Wang C, Lin K, Chang J, Sun J. The stimulation of osteogenic differentiation of mesenchymal stem cells and vascular endothelial growth factor secretion of endothelial cells by beta-

CaSiO3/beta-Ca3(PO4)2 scaffolds. J Biomed Mater Res. 2014; 102A:2096–104.
11. Lin K, Chang J, Shen R. The effect of powder properties on sintering, microstructure, mechanical strength and degradability of beta-tricalcium phosphate/calcium silicate composite bioceramics. Biomed Mater. 2009;4:065009.
12. Lin K, Zhai W, Ni S, Chang J, Zeng Y, Qian W. Study of the mechanical property and in vitro biocompatibility of CaSiO3 ceramics. Ceram Int. 2005;31:323–6.
13. Lin K, Chang J, Wang Z. Fabrication and the characterisation of the bioactivity and degradability of macroporous calcium silicate bioceramics in vitro. J Inorg Mater. 2005;20:692–8.
14. Agata de Sena L, Sanmartin de Almeida M, de Oliveira Fernandes V, Guerra Bretana R, Castro-Silva I, Granjeiro J, et al. Biocompatibility of wollastonite-poly(N-butyl-2-cyanoacrylate) composites. J Biomed Mater Res. 2014;102B:1121–9.
15. Yang Y, Zhang L, Yang G, Gao C, Gou Z. Preparation and characterization of multi-shell hollow biphase bioceramic microsphere composites. J Inorg Mater. 2014;29:650–6.
16. Zhang W, Shen Y, Pan H, Lin K, Liu X, Darvell BW, et al. Effects of strontium in modified biomaterials. Acta Biomater. 2011;7:800–8.
17. Lai W, Garino J, Flaitz C, Ducheyne P. Excretion of resorption products from bioactive glass implanted in rabbit muscle. J Biomed Mater Res. 2005;75A:398–407.
18. Lai W, Garino J, Ducheyne P. Silicon excretion from bioactive glass implanted in rabbit bone. Biomaterials. 2002;23:213–7.
19. Schwarz K. A bound form of silicon in glycosaminoglycans and polyuronides. Proc Natl Acad Sci USA. 1973;70:1608–12.
20. Dobbie J, Smith M. The silicon content of body fluids. Scott Med J. 1982;27:17–9.
21. Hamilton E, Minski M, Cleary J. The concentration and distribution of some stable elements in healthy human tissues from the United Kingdom: an environmental study. Sci Total Environ. 1973;1:341–74.
22. LeVier R. Distribution of silicon in the adult rat and rhesus monkey. Bioinorg Chem. 1975;4:109–15.
23. Kawanabe K, Yamamuro T, Nakamura T, Kotani S. Effects of injecting massive amounts of bioactive ceramics in mice. J Biomed Mater Res. 1991;25A:117–28.
24. Kawanabe K, Yamamuro T, Kotani S, Nakamura T. Acute nephrotoxicity as an adverse effect after intraperitoneal injection of massive amounts of bioactive ceramic powders in mice and rats. J Biomed Mater Res. 1992;26A:209–19.
25. Nagase M, Abe Y, Chigira M, Udagawa E. Toxicity of silica containing calcium-phosphate glasses demonstrated in mice. Biomaterials. 1992;13:172–5.
26. Lin K, Chang J, Zeng Y, Qian W. Preparation of macroporous calcium silicate ceramics. Mater Lett. 2004;58:2109–13.
27. Maehira F, Miyagi I, Eguchi Y. Effects of calcium sources and soluble silicate on bone metabolism and the related gene expression in mice. Nutrition. 2009;25:581–9.
28. Pietak AM, Reid JW, Stott MJ, Sayer M. Silicon substitution in the calcium phosphate bioceramics. Biomaterials. 2007;28: 4023–32.
29. Hoppe A, Guldal NS, Boccaccini AR. A review of the biological response to ionic dissolution products from bioactive glasses and glass-ceramics. Biomaterials. 2011;32:2757–74.
30. Zhai Q, Zhao S, Wang X, Li X, Li W, Zheng Y. Synthesis and characterization of bionic nano-silicon-substituted hydroxyapatite. J Inorg Mater. 2013;28:58–62.
31. D€orfler A, Detsch R, Romeis S, Schmidt J, Eisermann C, Peukert W, et al. Biocompatibility of submicron Bioglass® powders obtained by a top-down approach. J Biomed Mater Res. 2014;102B:952–61.